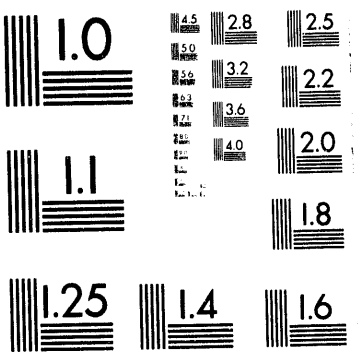
1.0
1.1
1.25
1.4
1.6
1.8
2.0
2.2
2.5
2.8
3.2
3.6
4.0
4.5
5.0
5.6
6.3
7.1

1 of 1

CONF-931079--22

SAND93-2261C

INTEGRATED ANALYSIS OF DCH IN SURRY[1]

Susan E. Dingman, Frederick T. Harper, Martin M. Pilch, Kenneth E. Washington

Sandia National Laboratories
Albuquerque, NM 87185

An evaluation of the key elements affecting Direct Containment Heating (DCH) was performed for the Surry plant. This involved determining the dominant high pressure core damage sequences, the probability of proceeding to vessel breach at high pressure, the DCH loads, and the containment strength. Each of these factors was evaluated separately, and then the results were combined to give the overall threat from DCH. The maximum containment failure probability by DCH for Surry is 10^{-3} when considering four base DCH scenarios and using the two-cell equilibrium (TCE) model. However, higher containment failure probabilities are estimated in sensitivity cases. When the depressurization and containment loads aspects are combined, the containment failure probability (conditional on station blackout sequence) is less than 10^{-2}. CONTAIN calculations were performed to provide insights regarding DCH phenomenological uncertainties and potential conservatisms in the TCE model. The CONTAIN calculations indicated that the TCE calculations were conservative for Surry and that the dominant factors were neglect of heat transfer to surroundings and complete combustion of hydrogen on DCH time scales.

1. INTRODUCTION

This work is part of a Nuclear Regulatory Commission (NRC) effort on Direct Containment Heating (DCH) resolution that involves three national laboratories and two universities. The key elements in the DCH resolution effort are: (1) the probability that sequences will proceed to vessel breach while at high pressure, rather than being depressurized by failures such as stuck-open relief valves, pump seal leaks, or hot leg failure; (2) the conditions of the reactor coolant system (RCS), containment, and lower head debris at the time of vessel breach; (3) the containment pressurization accompanying high pressure melt ejection (HPME); and (4) the containment strength. Resolution was approached by performing in-depth evaluations for the Surry and Zion plants, and developing a methodology for

---

[1] This work is supported by the U.S. Nuclear Regulatory Commission and is performed at Sandia National Laboratories, which is operated for the U.S. Department of Energy under Contract Number DE-AC04-94AL85000.

extrapolating this information to other pressurized water reactor (PWR) plants. Other papers for this 21st Water Reactor Safety Information Meeting focus on the analyses that were performed to estimate the probability of HPME occurring for various sequences at Surry and Zion and to estimate the containment failure probability for Zion for various HPME sequences. This paper focuses on an approach that addresses both of these aspects of the issue for Surry.

2. KEY PLANT CHARACTERISTICS

Surry Power Station, Unit 1 is a 2441 MWt Westinghouse pressurized water reactor (PWR). The reactor coolant system (RCS) has three U-tube steam generators and three reactor coolant pumps (RCPs). With the U-tube steam generator design, countercurrent natural circulation between the reactor pressure vessel (RPV) and steam generators is possible. This has been shown to have a large impact on the potential for temperature-induced failures during an accident. The pumps contain the older design of Westinghouse o-rings, which have a high probability of leaking during an accident involving loss of pump cooling.

Figure 1 shows a section through the Surry containment. The reactor cavity is connected to the surrounding subcompartments through a vertical chute. There is no connection between the sump and the reactor cavity at a low elevation in the Surry containment. Water from a pipe break in containment will flow to the sump. The reactor cavity will remain dry unless the containment sprays operate.

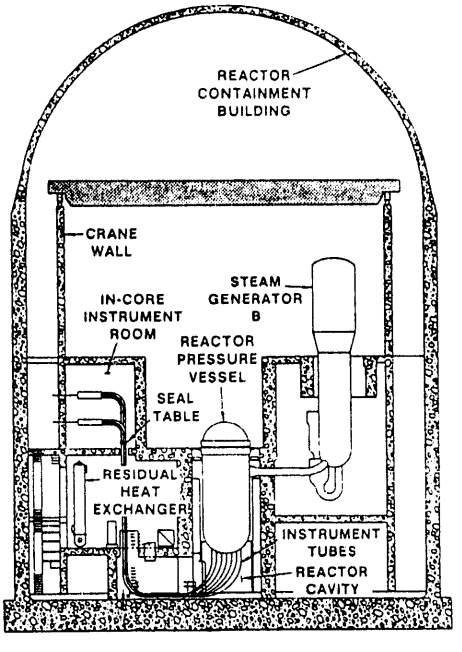

Figure 1 Surry containment schematic

The Surry containment is a cylinder with a hemispherical dome roof, both of which are steel-lined reinforced concrete. The foundation is a reinforced concrete slab. During operation, the containment is maintained about 5 psig below ambient atmospheric pressure.

3. DOMINANT HIGH PRESSURE CORE DAMAGE SEQUENCES

This section provides perspectives on the frequencies of accidents with high RCS pressures at core uncovery. Note that the pressure at the time of core uncovery can be either higher or lower than the pressure at the time of vessel breach (i.e., either depressurization or repressurization is possible following core damage). Those possibilities are discussed in the following section. The dominant core damage sequences from NUREG-1150 [1] are described. This information feeds into the development of four enveloping DCH scenarios that are actually used to calculate the DCH loads in Section 6.

In the discussions that follow, the plant will be discussed in terms of its internal event plant damage state (PDS) groups. These PDS groups represent the condition of the plant at the onset of core damage. The PDS groups are regroupings of the core damage accident sequences according to important characteristics that will affect the subsequent accident progression and the source term.

The mean internal event core damage frequency estimate for Surry in NUREG-1150 was 4.01E-5/yr, with 5% and 95% bounds of 6.75E-6/yr and 1.31E-4/yr, respectively. These values represent reasonably low values for internal event core damage frequency estimates. Of concern here is the fraction of accidents that are expected to be at high pressure at the onset of core damage. Within each PDS group, four RCS pressure ranges were considered:

System setpoint pressure	- 2500 psia (17.2 MPa)
High pressure	- 600 - 2000 psia (4.1 MPa - 13.8 MPa)
Intermediate pressure	- 200 - 600 psia (1.4 MPa - 4.1 MPa)
Low pressure	- < 200 psia (<1.4 MPa)

The dominant PDS groups with core uncovery at high pressure are the short term and long term station blackout sequences.

The long-term station blackout PDS group is the most likely PDS group, with a frequency of 2.2E-5 per reactor year. All of the sequences in this PDS are initiated by the loss of off-site power, followed by failure of on-site emergency ac power and successful operation of the turbine-driven portion of the auxiliary feedwater system. No containment systems are available. Core damage may occur in approximately seven hours due to battery depletion (four hours until battery depletion and an additional three hours until core uncovery), or sooner due to loss of coolant inventory resulting from a RCP seal loss-of-coolant accident (LOCA) or a stuck open power-operated relief valve (PORV). Any loss of RCS integrity prior to core damage involves no more than the equivalent of a small break LOCA. Source

Term Code Package calculations indicate that the pressure would be intermediate or higher for these conditions. The relative percentages of this PDS group falling in the system setpoint, high and intermediate pressure ranges are 54%, 13%, and 33%, respectively.

The frequency of the short-term station blackout PDS group is 5.4E-6 per reactor year. Short-term station blackout events begin with a loss of off-site and on-site ac power, but proceed rapidly due to failure of turbine-driven auxiliary feedwater. All of these sequences at Surry proceed to core damage with the RCS intact (i.e., at system setpoint pressure).

4. HPME PROBABILITY

The RCS could be depressurized between the times of core uncovery and vessel breach for the station blackout sequences through accident-induced ex-vessel pressure boundary failures. An assessment of the potential for HPME at Surry was recently completed [2]. This section contains a summary of that work; details are provided in the reference.

The probability of HPME for a short-term station blackout scenario at Surry was assessed by considering two issues:

1. What is the probability that the surge line or hot leg will fail and depressurize the RCS to a low pressure before lower head failure?

2. What are the probabilities of being at a low, intermediate, and high RCS pressure at the time of reactor vessel breach?

Similar to the treatment of DCH in NUREG-1150, low, intermediate, and high RCS pressures were taken to be pressures below 1.38 MPa, pressures between 1.38 and 6.89 MPa, and pressures above 6.89 MPa, respectively. SCDAP/RELAP5/MOD3 analyses coupled with sensitivity calculations and engineering judgement were used to obtain the probabilities listed in Tables 1 and 2 for the following short-term station blackout cases: (1) without RCP seal leaks (at full system pressure); (2) with seal leaks of 250 gpm per RCP; (3) with seal leaks of 480 gpm per RCP; and (4) with stuck-open/latched-open PORVs.

Table 1 Probabilities for a surge line or hot leg failure before lower head failure

Variations of Short-Term Station Blackout Scenario	Probability
1. without RCP seal leaks	0.98
2. with seal leaks of 250 gpm per RCP	0.98
3. with seal leaks of 480 gpm per RCP	0.0
4. with stuck-open/latched-open PORVs	1.0

Table 2 Probabilities of being at various RCS pressures at the time of reactor vessel breach

Variations of Short-Term Station Blackout Scenario	Probability, at vessel breach, for High RCS pressure (> 6.89 MPa)	Intermediate RCS pressure (1.38 - 6.89 MPa)	Low RCS pressure (< 1.38 MPa)
with hot leg or surge line failure before vessel breach	0.0	0.0	1.0
without RCP seal leaks	1.0	0.0	0.0
with seal leaks of 250 gpm per RCP	0.21	0.75	0.04
with seal leaks of 480 gpm per RCP	0.13	0.40	0.47
with stuck-open /latched-open PORVs	0.0	0.0	1.0

Probabilities listed in Table 1 account for potential uncertainties that could affect the timing of accident-induced failures as well as estimates of RCS depressurization that could follow ex-vessel failures. Probabilities listed in Table 2 include potentials for repressurizing (as a result of accumulator injections and/or debris/coolant heat transfer).

5. CONDITIONS AT VESSEL BREACH

The initial conditions for the DCH loads calculations were developed using the same rationale developed for Zion in NUREG/CR-6075.[2] That is, scenarios were constructed to envelop the physically possible behavior, with two major scenario bifurcations considered. The first major bifurcation reflects the possibility of two distinct melt progressions: (1) those involving the formation and failure of core blockages, allowing a coherent relocation of melt to the lower plenum, and (2) those involving the gradual relocation of melt to the lower plenum. The second major bifurcation involves the mode and timing of lower head failure, with penetration failures and creep rupture representing the extremes. The rationale used to develop initial conditions is described in NUREG/CR-6075.

A summary of the Surry DCH initial condition quantification is provided in Table 3. Probability density functions (PDFs) for the parameters are shown in Figures 2 through 4. The following equations are used to calculate parameters as indicated in the table.

---

[2] M. M. Pilch, H. Yan, T. G. Theofanous, The Probability of Containment Failure by Direct Containment Heating in Zion, NUREG/CR-6075, SAND93-1535, In preparation.

Table 3 Summary of Surry DCH initial condition quantification

Parameter	Crucible Formation		Gradual Relocation	
	I Penetration Failure	II Rupture	III Penetration Failure	IV Rupture
RCS Pressure (MPa)	8	8	8	8
RCS Temperature (K)	800	800	900	900
RPV Temperature (K)	600	1000	800	1000
Initial Hole Diameter (m)	0.0254	0.4	0.0254	0.4
Melt Temp. (K)	2800	2500	1900	2350
UO_2 Mass (MT*)	Fig. 2	Fig. 2	0	Fig. 2
Fraction Zr Oxidized	Fig. 3	Fig. 3	Fig. 3	Fig. 3
Zr Mass (MT)	0	Eq. 3	0	Eq. 5
ZrO_2 Mass (MT)	Eq. 1	Eq. 1	0	Eq. 1
Steel Mass (MT)	0	Eq. 4	Fig. 4	Eq. 6
Control Rod Material Mass (MT)	0	2.7	2.7	2.7
Containment H_2 Mole Fraction	Eq. 2	Eq. 2	Eq. 2	Eq. 2
Autoignition Temperature (K)	1100	1100	1100	1100
Melt Fraction Ejected into Cavity	1.0	1.0	0.90	0.90
Ejected Fraction Dispersed from Cavity	0.75	0.75	0.75	0.75
Dispersed Fraction through Seal Table Room, SG Vents and Annular Gap*	0.15	0.15	0.15	0.15
Containment Pressure (MPa)	0.22	0.22	0.22	0.22
Containment Temperature (K)	383	383	383	383

*MT = metric tons, SG = steam generator

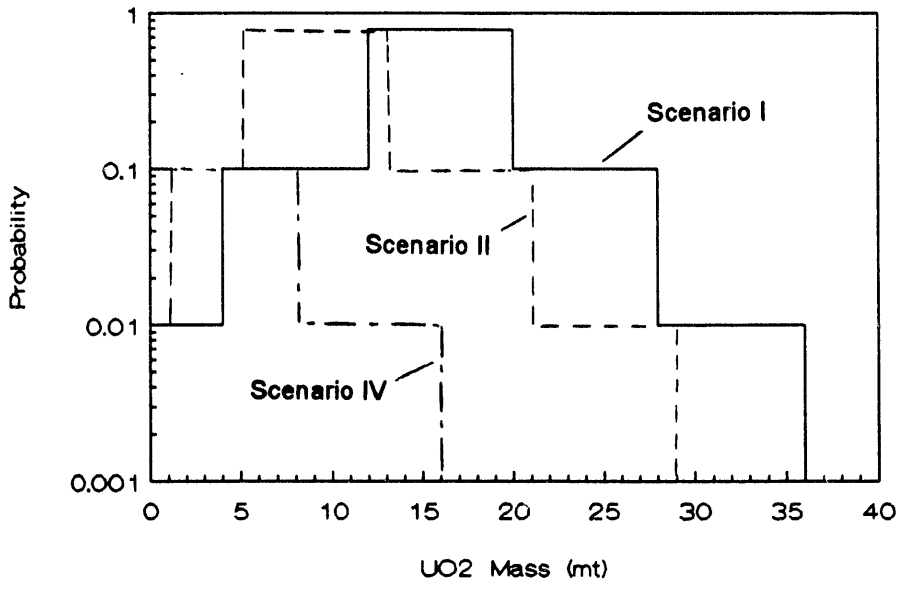

Figure 2 PDFs for UO_2 mass for Surry

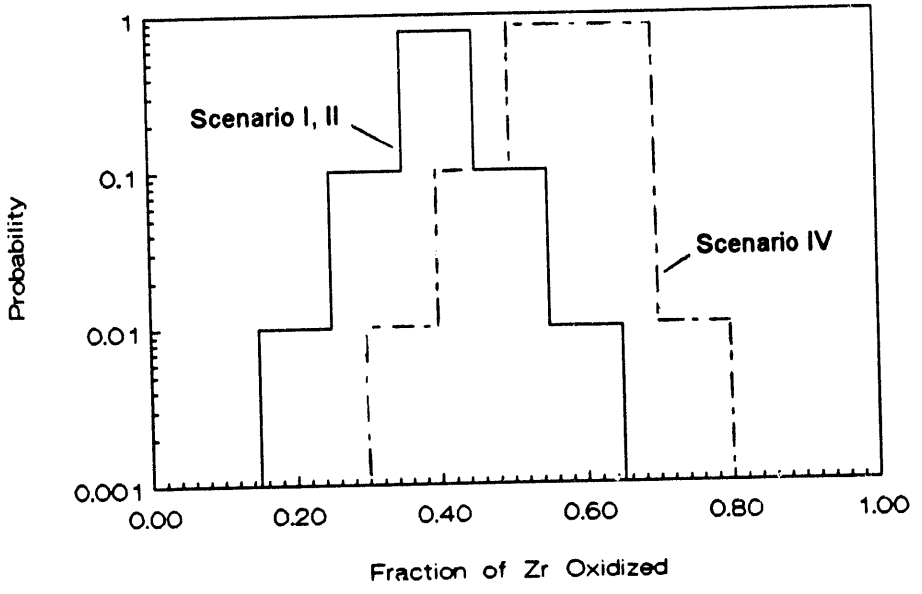

Figure 3 PDFs for fraction of Zr oxidized for Surry

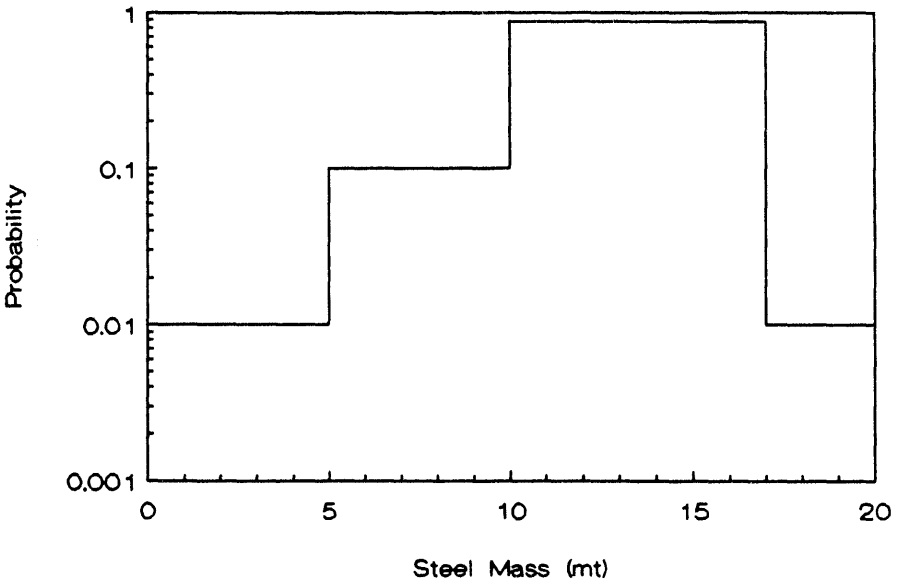

Figure 4 PDFs for steel mass for Surry

$$M_{ZrO2} = \frac{M_{UO2}}{M^o_{UO2}} M^o_{Zr} f_{Zr} \frac{123}{91} \quad , \tag{1}$$

where M_{ZrO2} is the mass of zirconium oxide, M_{UO2} is the molten mass of uranium dioxide (from Figure 2), M°_{UO2} is the initial mass of uranium dioxide in the core, M°_{Zr} is the initial mass of zirconium in the core, and f_{Zr} is the fraction of zirconium oxidized (from Figure 3).

$$X_{H2} = \frac{N_{H2}}{N^o_{ATM}} = \frac{\frac{2}{0.091} f_{Zr} M^o_{Zr}}{N^o_{ATM}} \quad , \tag{2}$$

where X_{H2} is the hydrogen mole fraction, N_{H2} is the moles of hydrogen in containment, and N°_{ATM} is the initial moles in containment.

$$M_{Zr} = 0.1\, M^o_{Zr}\, (1-f_{Zr}) \quad , \tag{3}$$

where M_{Zr} is the mass of zirconium ejected.

$$M_S = M_{S,LP} \frac{M_{UO2}+M_{ZrO2}+15\times10^3+M_{Zr}+M_{CRM}}{\rho_d \alpha_d V_{LP}} \quad , \tag{4}$$

where M_S is the mass of steel ejected, $M_{S,LP}$ is the initial mass of steel in the lower plenum, M_{CRM} is the mass of control rod material, V_{LP} is the volume of the lower plenum, and

values of α_d of 0.82 and ρ_d of 10400 kg/m^3 were used in the calculation.

$$M_{Zr} = \frac{M_{UO2}}{M^o_{UO2}} \; (1-f_{Zr}) M^o_{Zr} \tag{5}$$

$$M_s = \begin{cases} 20\ MT & if\ \ M_{UO2} > 0 \\ Fig.\ 4 & if\ \ M_{UO2} = 0 \end{cases} . \tag{6}$$

6. CONTAINMENT LOADS

The two-cell equilibrium (TCE) model (see NUREG/CR-6075) was used to calculate containment loads for the four DCH scenarios identified in the previous section. The dominant parameter in the TCE model is the coherence ratio, which is a measure of the fraction of the blowdown steam that can interact with the ejected debris. The correlation for the coherence ratio for the Surry geometry, which was developed using experimental data, was used in this analysis. To reflect uncertainties in the coherence ratio correlation, a distribution with a relative standard deviation of 16% was applied. The initial lower head failure hole size is listed in Table 3 for the four scenarios. The final hole size is calculated with the ablation model described in NUREG/CR-6075.

The EVNTRE [3] computer code, which was developed to evaluate complex event trees, was used to propagate the probability distributions for the initial conditions and the coherence ratio through the TCE model to give a distribution on peak containment pressure. The probability distributions were propagated through Monte Carlo sampling.

PDFs for the peak containment pressure for the four scenarios are plotted in Figure 5. Examination of these and other results led to the following observations:

1. Scenario I is very benign, Scenarios II and III produce similar and slightly higher loads, and Scenario IV is the most severe.

2. Calculated temperatures do not exceed 950 K except in Scenario IV; thus, burning of pre-existing hydrogen does not contribute significantly to the DCH loads. Some hydrogen is entrained and burned in the DCH diffusion flame.

7. STRUCTURAL STRENGTH

The Surry containment fragility curve [4] that was developed for NUREG-1150, and subsequently used in the Surry individual plant examination (IPE), was used for this analysis. It was based on the input of four experts who were asked to determine what distribution

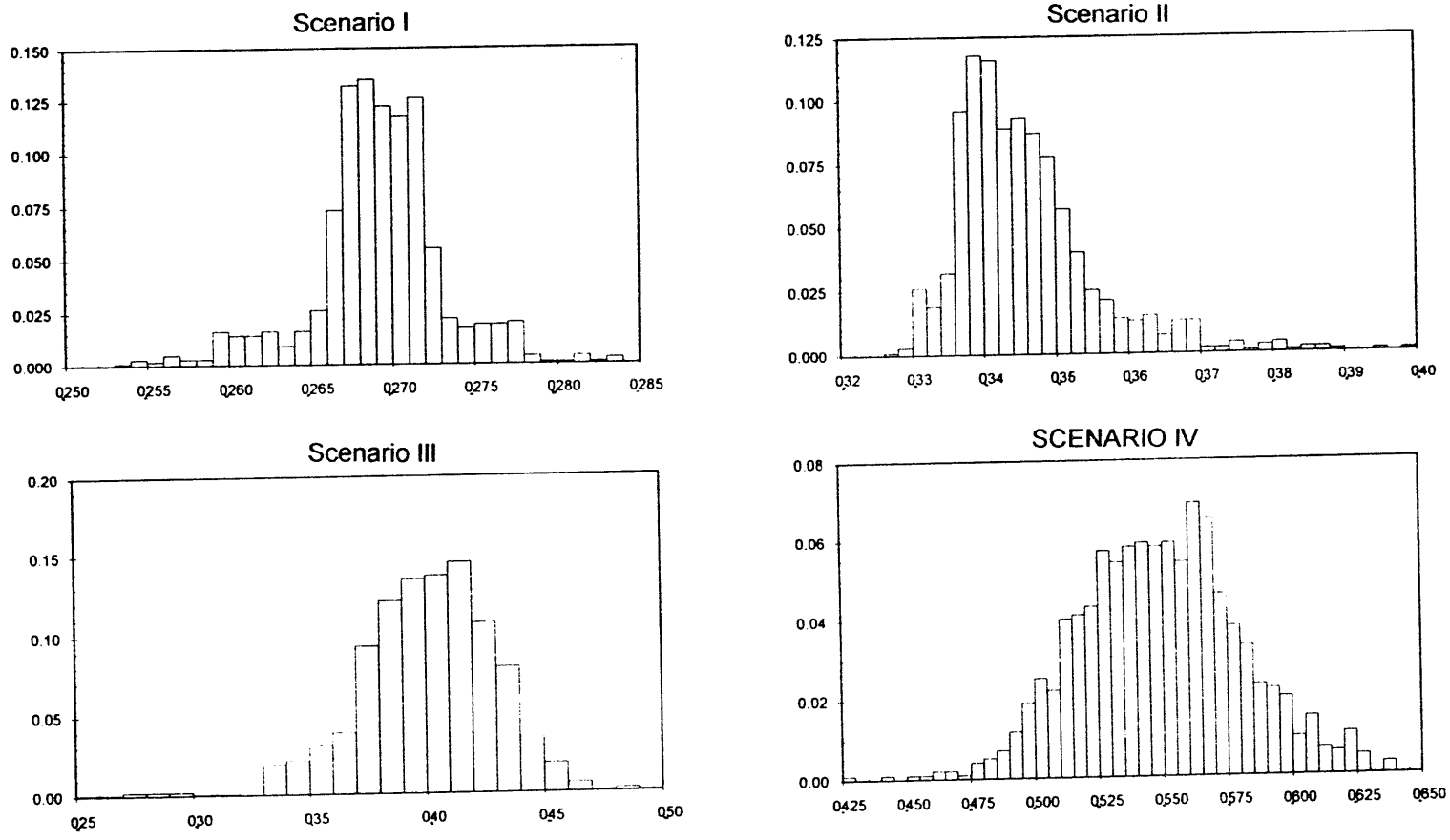

Figure 5 Calculated distribution for containment pressure (MPa) for Surry

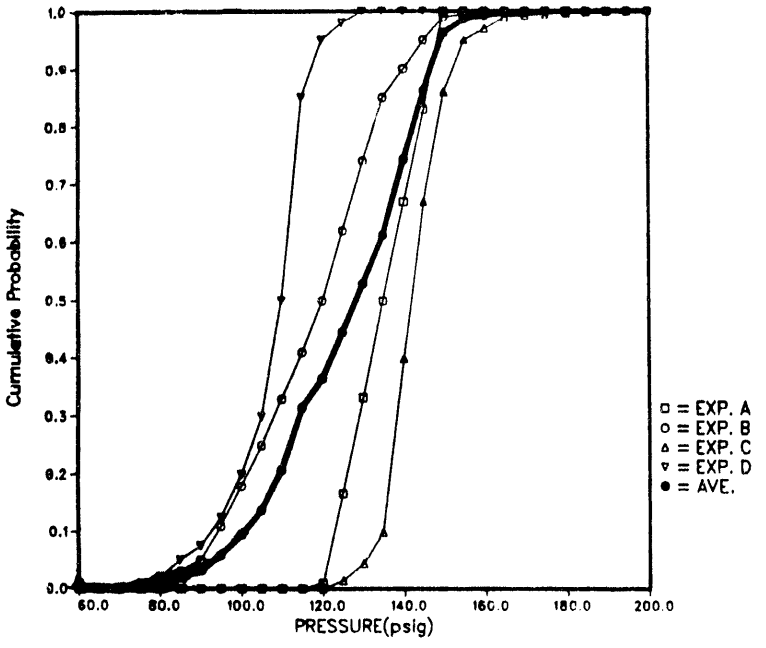

Figure 6 Cumulative failure probabilities

characterizes the failure pressure for static loading of the Surry containment and what conditional probabilities describe the failure modes at each pressure. Figure 6 shows the distributions of the four experts and the aggregate distribution for total cumulative failure probability.

8. CONTAINMENT FAILURE PROBABILITY

The DCH loads were convolved with the fragility curve to give containment failure probabilities for the four DCH scenarios. The calculations were carried out using the EVNTRE computer code with Monte Carlo sampling.

The containment loads curve does not intersect the containment fragility curve for DCH Scenarios I through III. Thus, the probability of containment failure is 0. for these three scenarios. There is a slight intersection for Scenario IV, with a containment failure probability of less than 0.001.

The sensitivity studies established in NUREG/CR-6075 for Zion were also performed for Surry. The sensitivities examined are:

1. Hydrogen autoignition temperature of 950 K.

2. Total debris transport to the dome (annular gap, seal table room, and steam generator vents) increased to 20 percent.

3. Initial hole size for rupture scenarios (II, IV) increased to 0.7 m.

4. Pressure increased to 16 MPa.

In NUREG/CR-6075, the melt conditions for Zion were altered for Scenario IV for the full system pressure studies. The stated justification was that the quantity, composition, and temperature of the melt is quite sensitive to the timing of bottom head rupture, which would be expected to be earlier for full pressure scenarios than for the 8 MPa case. It was argued that no oxide would be molten, and that consequently, only molten steel with a distribution similar to Scenario III would be present. This same approach was adopted for the Surry full pressure sensitivity study. Because of the high driving pressures at full system pressure, melt dispersal from the cavity is assumed to be complete. Lastly, 20% of all hydrogen produced during core degradation will be retained in the RCS with the remaining 80% preexisting in the containment atmosphere prior to vessel failure.

The sensitivity studies include all single and pairwise combinations among these four parameters (where appropriate), one in which all four parameters were varied simultaneously, and several triplet combinations. The containment failure probability was less than 10^{-3} for Scenarios I through III for all of these combinations. Higher containment failure probabilities were calculated for Scenario IV. The results are listed in Table 4. The table is organized as a matrix where repetitious elements are shaded. Single variations from the base quantifications lie along the diagonal of the sensitivity matrix. The largest sensitivity is seen for the full pressure case, which has a containment failure probability of 0.05. The two way combinations are included in the off diagonal elements of the table. The greatest sensitivity is for the full pressure scenario with a 0.7 m hole in the lower head. For this case, the containment failure probability is 0.21. Simultaneous variations of all four parameters results in a containment failure probability of 0.24.

Next, event trees were used to combine the individual probabilities for induced RCS failures and depressurization, giving the probability of vessel breach occurring at various pressure levels for particular sequences. The long-term and short-term station blackout sequences that were identified in NUREG-1150 were evaluated. Probabilities for a stuck-open PORV or pump seal leak were obtained from the NUREG-1150 study. The event tree used in the evaluation is shown in Figure 7. The mean probabilities for the event tree branches are indicated on the figure.

The probability of vessel breach occurring at various pressure levels was calculated using the EVNTRE code and latin hypercube sampling. The results for the long-term and short-term station blackout sequences are shown in Table 5.

Table 4 Scenario IV - sensitivity studies

	Containment Failure Probability (CFP)			
	Autoignition 950 K	Dome Transport 20%	Initial Hole Size, 0.7 m	Full Pressure 16 MPa
Autoignition 950 K	0.015			
Dome Transport 20%	0.019	$<10^{-3}$		
Initial Hole Size, 0.7 m	0.05	0.01	0.005	
Full Pressure 16 MPa	0.11	0.06	0.21	0.05

Simultaneous combination of first three sensitivities at 8 MPa; CFP = 0.061.
Simultaneous combination of four sensitivities at 16 MPa; CFP = 0.24.

For the long-term station blackout sequence, the probability of being at system setpoint pressure ($6x10^{-3}$) can be combined with the highest containment failure probability from the Scenario IV sensitivity studies (.24) to give a bounding containment failure probability of $1x10^{-3}$ for the full pressure scenarios. Similarly, the probability of vessel breach at high pressure (.055) can be combined with the highest containment failure probability for the 8 MPa Scenario IV cases (.061) to give a bounding containment failure probability for high pressure scenarios of $3x10^{-3}$. Combining the bounding containment failure probabilities for the system setpoint and high pressure scenarios gives a bounding containment failure probability for the long-term station blackout sequence of $5x10^{-3}$. This is well below 0.1, which has been established by NRC as the criterion for unacceptably low containment failure probability. The probabilities of being at system setpoint or high pressure are even lower for the short-term station blackout scenario, giving a bounding containment failure probability of $9x10^{-4}$.

In summary, the maximum containment failure probability by DCH for Surry is 10^{-3} in the four base scenarios. However, the sensitivity cases indicate higher containment failure probabilities for Scenario IV. When the depressurization and containment loads aspects are combined, the containment failure probability is less than 10^{-2} even for the sensitivity cases of Scenario IV.

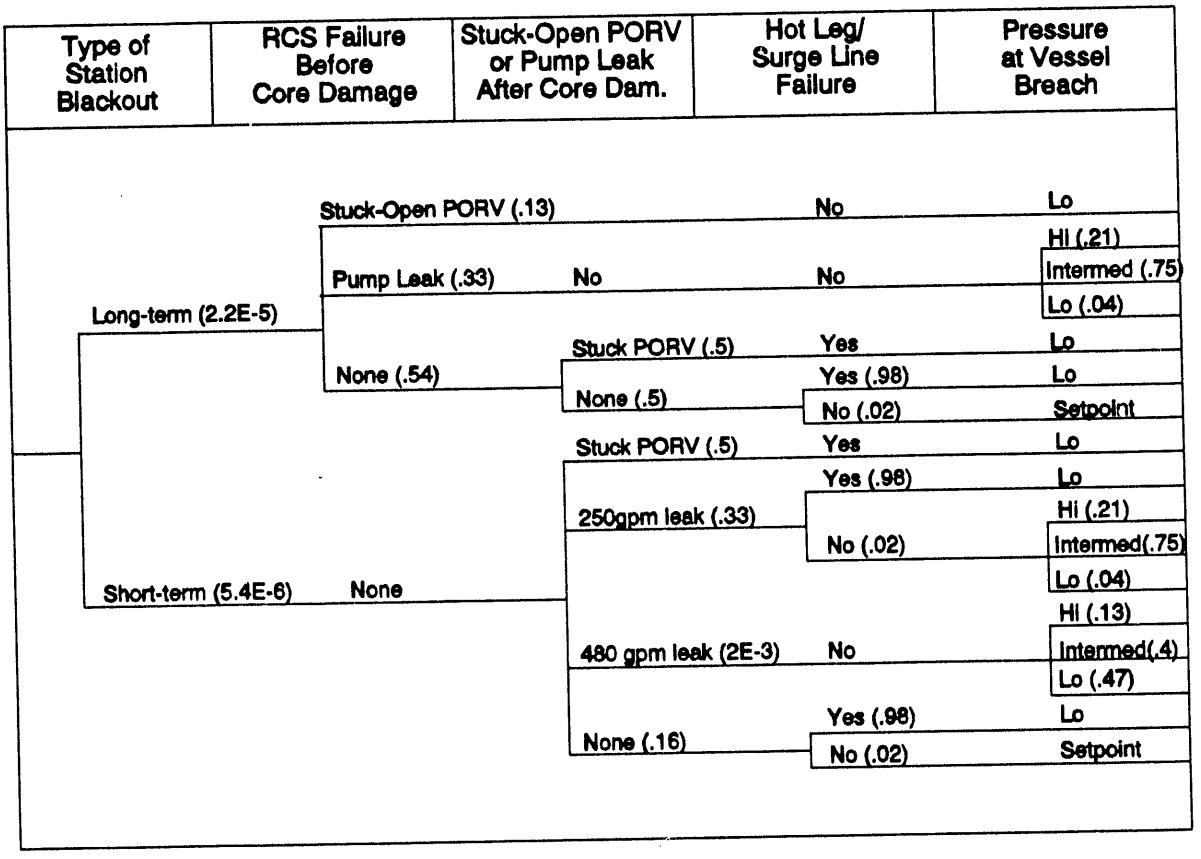

Figure 7 Event tree for assessing HPME probability for Surry

Table 5 HPME probabilities for Surry

Pressure Range	Probability of Vessel Breach in Pressure Range	
	Long-term Station Blackout	Short-term Station Blackout
System Setpoint (16 MPa)	0.0058	0.0023
High (6.89 - 16 MPa)	0.055	0.0034
Intermediate (1.38 - 6.89 MPa)	0.20	0.012
Low (< 1.38 MPa)	0.74	0.98

9. CONTAINMENT LOADS USING CONTAIN

This section describes the application of CONTAIN to the quantification of DCH containment loads for Surry. The purpose of these calculations is to provide insight into the degree of conservatism obtained when loads in the Surry plant are predicted using the simpler TCE model. To accomplish this goal, many of the same assumptions used in TCE for DCH processes that are poorly understood are used in the CONTAIN analyses presented here. For processes that are more completely understood, and where CONTAIN provides a defensible mechanistic approach, that approach is used and will therefore differ from the TCE approach. The CONTAIN DCH models are documented in a series of letter reports to the NRC.[3]

Two specific variations of DCH Scenario IV have been identified for providing insights into best-estimate DCH loads using CONTAIN: (1) a fully pressurized (16 MPa) scenario with a 0.7 m initial hole size, and (2) a partially pressurized (8 MPa) scenario with a 0.4 m initial hole size. For these scenarios the adiabatic TCE model predicts large enough loads that questions have arisen as to whether there are excessive conservatisms that can be relaxed through the use of a more detailed code such as CONTAIN. Examples of important conservatisms that can be relaxed by using CONTAIN include: (1) chemical and heat transfer kinetic limitations, (2) transport time and combustion rate of hydrogen, and (3) heat losses to structural surroundings. The CONTAIN calculations that were performed and that are presented here emphasize capturing these mitigating effects, while attempting to ensure that the poorly understood processes be represented in a conservative manner (i.e., comparable to the TCE model).

The Surry containment was represented using a 16 cell nodalization plus a cell for the RCS to generate the gas blowdown. The key modeling assumptions and related input parameters used in the Surry plant calculations are summarized in Table 6. A more in depth description of this analysis methodology is provided in the footnoted references below.[4,5]

The base case initial and boundary conditions and the various sensitivity cases that were run are summarized in Table 7 along with the key results obtained. The base case results are given by the columns named SY11 (16 MPa) and SY21 (8 MPa). The effect of burning the

---

[3] K. E. Washington, *et al.*, C110U Code Change Document; C110Y Code Change Document; R. O. Griffith, *et al.*, C110Z Code Change Document. Letter reports to NRC; Sandia National Laboratories, 1993.

[4] K. E. Washington and D. C. Williams; presentation to the 3rd meeting of the CONTAIN peer review, Rockville, MD, January 1994.

[5] D. C. Williams, K. E. Washington, and R. O. Griffith, CONTAIN DCH Assessment, In Preparation.

Table 6 Summary of CONTAIN DCH calculational methodology

Process	Approach	Notes
RPV Dispersal	User specified as linear over 1.0 s onto cavity floor	Little effect on pressure rise
Entrainment Fraction	100% (16 MPa case) 75% (8 MPa case)	Same as TCE
Entrainment Rate	User specified to match Pilch coherence ration correlation	Equivalent to TCE
Debris Particle Size	1 mm mass mean, lognormal distribution over 5 size bins	As observed in experiments
Trapping	Time of flight, Kutateladze CONTAIN model (see footnote 2 on previous page)	Resulted in ~15% carryover
Diffusion Flame	Burn all hydrogen flowing into dome and entrain some pre-existing hydrogen	Model same as TCE treatment
Volumetric Burning	Equivalent to 5 m/s deflagration above autoignition temperature	950 K base case 700 K sensitivity

pre-existing hydrogen in the dome volumetrically is addressed by cases SY12 (16 MPa) and SY22 (8 MPa). The effect of non-airborne debris interactions (at 75% dispersal for the 8 MPa scenario) is addressed by case SY23. The importance of heat loss to structures is addressed by case SY13. Not shown on this table are the results of the sensitivity cases exploring the effects of co-dispersed water for the 8 MPa scenario. These results are shown in Figure 8.

A few key points are noted concerning the results shown in Table 7. First it is pointed out that the autoignition is not predicted to occur when the threshold is set at 950 K; therefore, identical results would be obtained using a 1100 K threshold. The 700 K cases were performed to address three potential non-conservatisms. First, they address the question of CONTAIN's ability to accurately predict temperatures under such conditions. That is, if portions of the dome are hotter than the well-mixed prediction given by a CONTAIN calculation, one might expect the pre-existing hydrogen to partially burn. Second, they address the uncertainty associated with the high temperature recombination rate. Third, the amount of pre-existing hydrogen presents a nearly-flammable mixture, and under such conditions there are questions as to whether DCH conditions would be sufficiently severe to bring the mixture into a flammable regime. The Chemkin code could be used to address these uncertainties more mechanistically; however, the effective 5 m/s burning rate above 700 K is believed to be conservative.

Table 7 Summary of CONTAIN Surry DCH predictions

Parameter	SY21	SY22	SY23	SY11	SY12	SY13
RCS Pressure (MPa)	8	8	8	16	16	16
Initial/Final Hole Diameter (m)	0.4 0.53	0.4 0.53	0.4 0.53	0.7 0.72	0.7 0.72	0.7 0.72
Melt Temperature (K)	2350	2350	2350	1900	1900	1900
UO2/Zr/ZrO2 Steel/Control Rod Material Mass (MT)	8/.5/1.5 20/3	8/.5/1.5 20/3	8/.5/1.5 20/3	0/0/0 16/3	0/0/0 16/3	0/0/0 16/3
Autoignition T	950	**700**	**700**	950	**700**	**700**
Heat Sinks	Active	Active	Active	Active	Active	**None**
Non-airborne	0.01 m	0.01 m	**None**	0.01 m	0.01 m	0.01 m
Peak Pressure (MPa)	**0.49**	**0.64**	**0.62**	**0.55**	**0.66**	**~0.85***
Dome Peak T	731	1169	1157	786	1108	>1330*
Carryover fraction	13%	12%	13%	16%	16%	16%
h2 burned @5s (kg)	180	323	306	285	434	432
h2 burned @20 s (kg)	268	645	635	313	665	704
h2 produced (kg)	395	399	257	482	480	480

*The pressure and temperature were slightly increasing when the calculation was terminated at 20 s

Comparing the results of cases SY11 to SY12 and case SY21 to SY22, one can see that autoignition of the pre-existing hydrogen does result in a noticeable increase in the predicted loads. An interesting point, however, is that for the 16 MPa case, even when autoignition above 700 K is assumed, the predicted loads are below the comparable 0.91 MPa TCE result. The main reason for the lower predicted loads can be seen by comparing case SY12 to SY13, where the effect of heat losses to structures is greater than the effect of burning the pre-existing hydrogen for this scenario.

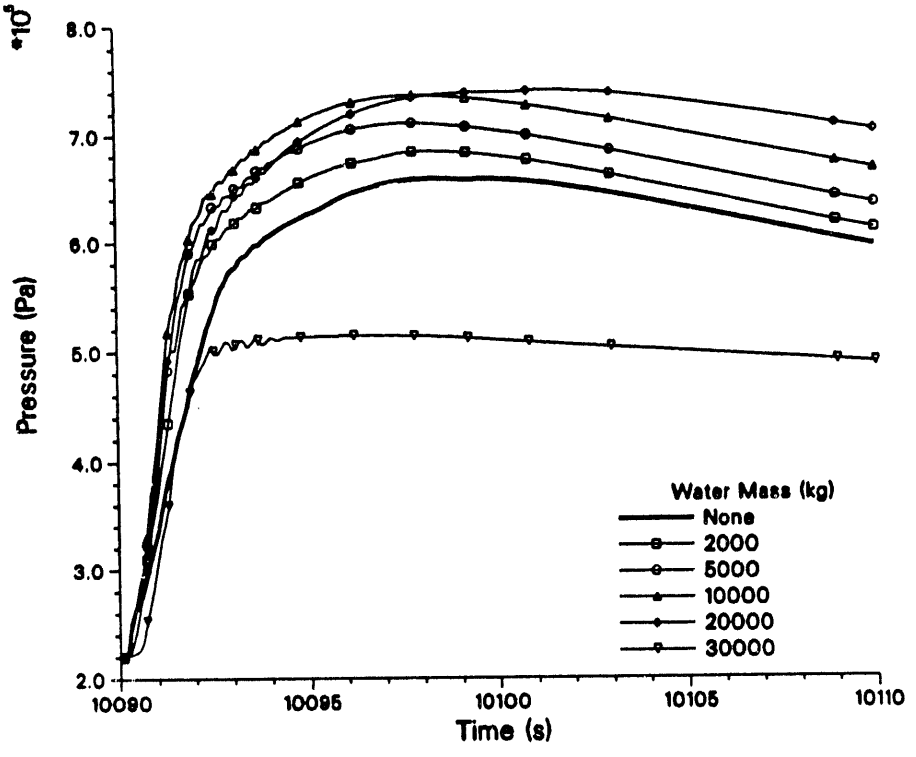

Figure 8 CONTAIN sensitivity cases for co-dispersed water

An interesting insight can be gained by examining the difference between the hydrogen burned numbers at 5 seconds after vessel breach, and at 20 seconds after vessel breach. The difference between these numbers for the 700 K cases clearly shows that much of the hydrogen recombination is not occurring on a time scale to affect peak DCH loads. Note that the hydrogen produced is essentially the same between cases SY11 and SY12. Of course when heat sinks are removed, then the extra hydrogen burning does contribute to the peak predicted loads.

Another useful insight is gained by comparing the hydrogen production results of case SY22 to case SY23. From this comparison one can see that the 25% non-airborne debris remaining in the cavity can result in a significant increase in the hydrogen production if it does react in the cavity. This is consistent with the trend that was seen in experiment analyses using CONTAIN (see footnote 4 for reference). Note, however, that the peak loads are similar for these two cases. This is because the extra hydrogen generated in case SY23 does not burn because of oxygen starvation in the lower compartments. This is confirmed by comparing the amount of hydrogen burned for the two cases. The loads do go down slightly in case SY23 because of less hydrogen burning before 5 seconds.

It is interesting to note that the debris carryover results shown on Table 7 agree with the assumed value for debris carryover used in the TCE analysis. Note that this result was obtained without performing any numerical experimentation with the trapping or slip models; the fractions just happened to turn out close to the assumed 15% value used in the TCE analysis. This result is desirable because it allows us to compare other aspects of the modeling on an equal footing with the TCE model and therefore enable insights into the conservatism included to be more straightforwardly extracted.

The final insight discussed is the effect of co-dispersed water shown in Figure 8. These results reiterate lessons from earlier CONTAIN analyses [5] where it was shown that small amounts of co-dispersed participating water can result in increased loads, and only at much larger masses will the quenching effect of the co-dispersed water result in a reduction in the predicted loads. The mass of water where quenching begins to be observed is largely governed by whether the produced hydrogen is allowed to burn as a diffusion flame. In the results shown in Figure 8, all hydrogen was allowed to burn above 400 K, and the turnaround point occurs at about 20,000 kg. If hydrogen is allowed to burn only above 1000 K in the diffusion flame, the turnaround occurs at about 7500 kg (not shown). Such small amounts of water required to observe quenching are consistent with previous CONTAIN results since the present analyses involve smaller melt masses, and because debris trapping and transport are being treated more realistically in the present generation of CONTAIN analyses.

REFERENCES

1. U.S. Nuclear Regulatory Commission, Severe Accident Risks: An Assessment for Five U.S. Nuclear Power Plants, NUREG-1150, December 1990.

2. Knudson, D. L., and Dobbe, C. A., Assessment of the Potential for High-Pressure Melt Ejection Resulting from a Surry Station Blackout Transient, NUREG/CR-5949, EGG-2689, November 1993.

3. Griesmeyer, J. M., and Smith, L. N., A Reference Manual for the Event Progression Analysis Code (EVNTRE), NUREG/CR-5174, SAND88-1607, September 1989.

4. Breeding, R.J., *et al.*, Evaluation of Severe Accident Risks: Quantification of Major Input Parameters, NUREG/CR-4551, SAND86-1309, Vol. 2, Rev. 1, Part 3, March 1992.

5. Williams, D. C., *et al.*, Containment Loads Due to Direct Containment Heating and Associated Hydrogen Behavior: Analysis and Calculations with the CONTAIN Code, NUREG/CR-4896, SAND87-0633, May 1987.

DISCLAIMER

DATE FILMED

4/25/94

END